
Faculty of Science

Faculty Publications

This is a post-print version of the following article:

Photodeamination Reaction Mechanism in Aminomethyl *p*-Cresol Derivatives:
Different Reactivity of Amines and Ammonium Salts

Dani Skalamera, Cornelia Bohne, Stephan Landgraf & Nikola Basaric

October 2015

The final publication is available via American Chemical Society Publications at:

<https://doi.org/10.1021/acs.joc.5b01991>

Citation for this paper:

Skalamera, D., Bohne, C., Landgraf, S., & Basaric, N. (2015). Photodeamination Reaction Mechanism in Aminomethyl *p*-Cresol Derivatives: Different Reactivity of Amines and Ammonium Salts. *Journal of Organic Chemistry*, 80(21), 10817-10828.
<https://doi.org/10.1021/acs.joc.5b01991>.

Photodeamination reaction mechanism in aminomethyl *p*-cresol derivatives: different reactivity of amines and ammonium salts

Dani Škalamera,[†] Cornelia Bohne,[‡] Stephan Landgraf[§] and Nikola Basarić,^{†*}

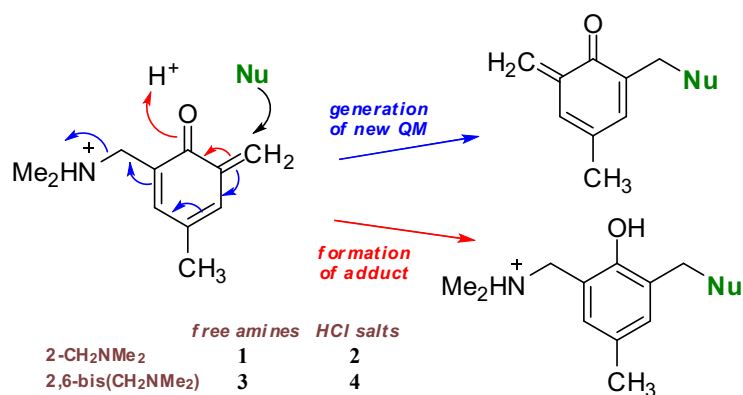
[†] Department of Organic Chemistry and Biochemistry, Ruđer Bošković Institute, Bijenička cesta 54, 10 000 Zagreb, Croatia. Fax: + 385 1 4680 195; Tel: +385 1 4561 141

[‡] Department of Chemistry, University of Victoria, Box 3065 STN CSC, Victoria BC, V8W 3V6, Canada.

[§] Institute of Physical and Theoretical Chemistry, Graz University of Technology, Stremayrgasse 9, A-8010 Graz, Austria

Corresponding author's E-mail address: NB nbasarić@irb.hr

Graphical abstract



Abstract: Derivatives of *p*-cresol **1-4** were synthesized and their photochemical reactivity, acid-base and photophysical properties were investigated. The photoreactivity of amines **1** and **3** is

different from that for the corresponding ammonium salts **2** and **4**. All compounds have low fluorescence quantum yields because the excited states undergo deamination reactions and for all cresols the formation of quinone methides (QMs) was observed by laser flash photolysis. The reactivity observed is a consequence of the higher acidity of the S₁ states of these *p*-cresols and the ability for excited-state intramolecular proton transfer (ESIPT) to occur in the case of **1** and **3**, but not for salts **2** and **4**. In aqueous solvent deamination depends largely on the prototropic form of the molecule. The most efficient deamination takes place when monoamine is in the zwitterionic form (pH 9-11) or diamine is in the monocationic form (pH 7-9). **QM1**, **QM3** and **QM4** react with nucleophiles and **QM1** exhibits shorter lifetime when formed from **1** (τ in CH₃CN = 5 ms) then from **2** (τ in CH₃CN = 200 ms) due to the reaction with eliminated dimethylamine, which acts as a nucleophile in the case of **QM1**. Bifunctional **QM4** undergoes two types of reactions with nucleophiles, giving adducts or new QM species. The mechanistic diversity uncovered is of significance to biological systems, such as for the use of bifunctional QMs to achieve DNA cross-linking.

Key words: excited state proton transfer (ESPT), quinone methides, laser flash photolysis, photodeamination

Introduction

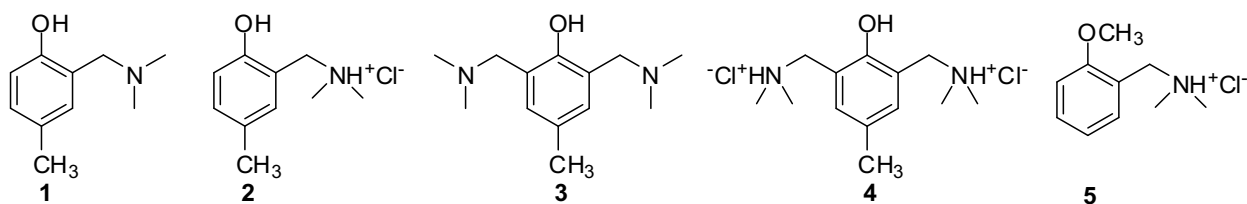
Quinone methides (QMs) are reactive intermediates encountered in the chemistry and photochemistry of phenols.¹ QMs have biological activity,^{2,3,4,5,6} and they were shown to react with amino acids,^{7,8} proteins,⁹ nucleobases^{10,11,12} and DNA.^{13,14,15,16} Some antineoplastic antibiotics such as mitomycin exhibit antiproliferative action on metabolic formation of QMs and

subsequent alkylation of DNA.^{17,18,19} Moreover, we have recently demonstrated that antiproliferative activity of photogenerated QMs stems from their reaction with intracellular proteins rather than with DNA.²⁰

QMs can be generated in thermal reactions including oxidation of phenols,²¹ dehydration from hydroxybenzyl alcohols,^{22,23} elimination of nitriles from 1,2-benzoxazines,²⁴ and fluoride induced desilylation.^{14,15} Photochemical methods enable access to QMs under much milder conditions and provide spatial and temporal control of the process, which is particularly appealing in biological systems.^{4,5} The photochemical methods to generate QMs rely on the photoelimination of HF,²⁵ or acetic acid,²⁶ photodehydration,^{27,28} or phototautomerization of suitably substituted phenols²⁹ or naphthols,³⁰ and photohydration of alkenes.³¹ The most common photochemical method to generate QMs in biological systems is photodeamination from the Mannich salts of the corresponding phenols,^{8,32} which can also be facilitated in an intramolecular photoinduced electron transfer reaction with naphthalene diimide as photooxidizing agent.³³ Photodeamination of Mannich salts has recently been applied in the investigation of biological activity of QMs,^{34,35} and the ability of naphthalenediimide QM derivatives to selectively target guanine quadruplex structures has been demonstrated.^{36,37,38}

In spite of numerous biological implications of photodeamination, a systematic mechanistic investigation of QM formation through deamination reactions and QM reactivity is lacking. Therefore, it is of pivotal importance to investigate the mechanism of QM formation in deamination, as well as reactivity of the corresponding QMs. Herein we report a mechanistic study of the photodeamination for a series of four cresol derivatives **1-4**. The molecules were designed to probe for the effect of the nitrogen protonation (**1** and **3** vs. salts **2** and **4**) and to determine the differences between mono- and di-substitution (**1** and **2** vs. **3** and **4**) on the

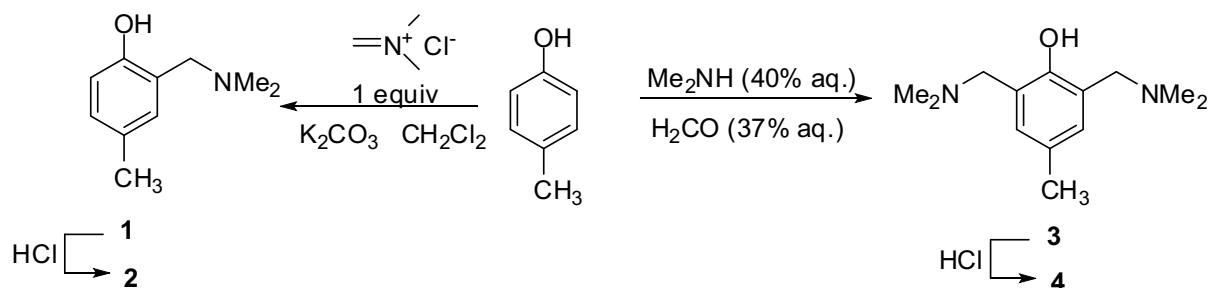
efficiency of QM generation and its reactivity. Bifunctional **3** and **4** are potentially applicable for DNA cross-linking and it is important to understand the difference in reactivity compared to **1** and **2**. The photochemical reactivity of **1-4** was investigated by preparative irradiations and compared to the reactivity of ether **5** that cannot give QM. Photophysical properties were investigated by fluorescence spectroscopy, whereas formation of the QMs and other potential reactive intermediates was probed by laser flash photolysis (LFP).



Results

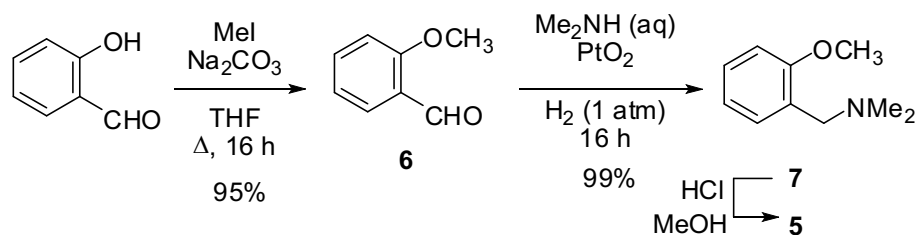
Synthesis

Cresol derivatives **1-4** were prepared in high yields (87-93%) by a simple procedure from *p*-cresol and Eschenmoser's salt which was used in equimolar ratio to form **1**, or prepared in excess *in situ* to yield **3** (Scheme 1). *p*-Cresol was chosen as a substrate in the Mannich reaction so that the methyl group prevented the reaction at the *para*-position yielding only **1** or **3**, and facilitated the purification. The free bases were transformed to the corresponding salts **2** and **4** in ethereal HCl solutions.



Scheme 1. Preparation of 1-4

Ether **5**³⁹ was prepared in excellent yield from salicylaldehyde (Scheme 2), which was methylated to **6**.⁴⁰ A reaction of **6** with dimethylamine, and subsequent hydrogenation of imine on PtO₂ furnished **7** that was transformed into salt **5**.



Scheme 2. Synthesis of ether **5**.

UV-vis and fluorescence measurements

Compounds **1-4** were characterized in different solvents by absorption and fluorescence spectroscopy (Fig. 1 and Figs. S1-S12 in the Supporting Information). Absorption spectra are about 10 nm bathochromically shifted compared to the phenol S₀→S₁ absorption.⁴¹ Fluorescence spectra taken in CH₃CN are structureless with one emission band for **2** and **4**, and dual emission for **1** and **3** (Fig 1). The emission at 308-318 nm is attributed to the fluorescence of phenol, whereas the band at 370 nm, seen only for **1** and **3**, corresponds to the emission of phenolate formed by excited state intramolecular proton transfer (ESIPT) from acidic phenol OH to the

basic dimethylamine nitrogen (Table 1). Upon electronic excitation phenols exhibit enhanced acidity (unsubstituted phenol $pK_a^* = 3.6$).^{42,43} Since the basic amine nitrogen is in close proximity to phenol OH in **1** and **3**, but not in **2** and **4** wherein the amine groups are protonated, excitation of **1** and **3** to S_1 leads to ESIPT, as demonstrated in similar precedent examples.^{44,45,46,47}

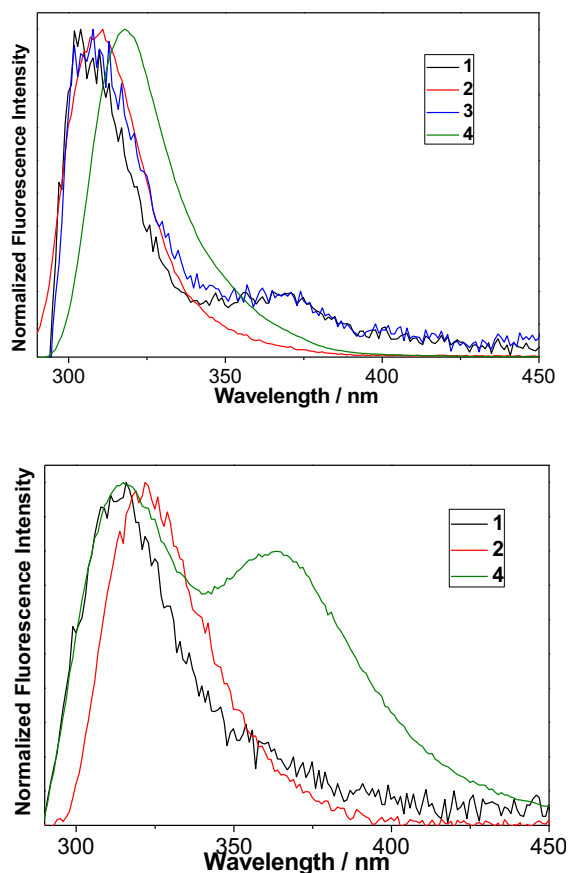


Figure 1. Normalized fluorescence spectra at the emission maxima of **1-4** in CH₃CN (top, $\lambda_{ex} = 260$ nm) and CH₃CN-H₂O (1:1) for **1**, **2** and **4** (bottom, $\lambda_{ex} = 260$ nm).

Quantum yields of fluorescence for **1-4** were measured by use of anisole in cyclohexane ($\Phi_f = 0.29$)⁴⁸ as a reference (eq. S1 in the Supporting Information). Generally, all compounds are very weakly fluorescent in CH₃CN with the fluorescent quantum yields in the range 0.001-0.05, indicating efficient non-radiative deactivation from S₁ (Table 1). In addition, Φ_f is approximately ten times lower for amines **1** and **3** when compared to **2** and **4** due to deactivation by ESIPT. We attempted to measure fluorescence decays of **1-4** by time-correlated single photon counting (SPC). However, due to the very weak fluorescence, multiexponential decays with contribution of short decay components (< 100 ps), and high photochemical reactivity of the molecules, no reliable time-resolved data could be obtained on the setup used.

Table 1. Maximum in the absorption and emission spectra (λ_{\max}) and fluorescence quantum yields (Φ_f) of **1-4** in acetonitrile.

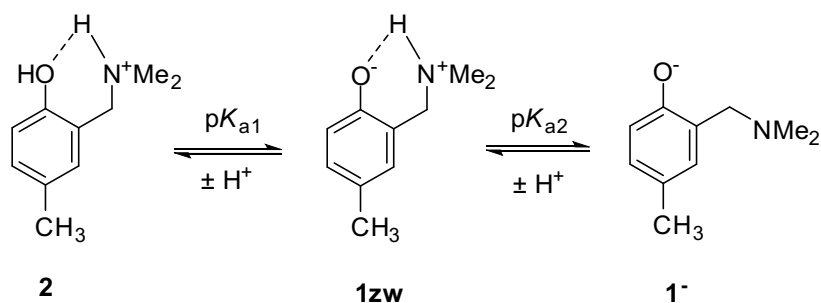
	$\lambda_{\max} / \text{nm}^a$	$\lambda_{\max} / \text{nm}^b$	$\Phi_f (\text{CH}_3\text{CN})^c$
1	283	308	$(1.5 \pm 0.5) \times 10^{-3}$
		370 (shoulder)	
2	286	310	$(12.6 \pm 0.2) \times 10^{-3}$
3	283	308	$(3 \pm 1) \times 10^{-3}$
		370 (shoulder)	
4	286	318	$(52.2 \pm 0.8) \times 10^{-3}$

^a Maximum in the absorption spectrum. ^b Maximum in the emission spectrum ($\lambda_{\text{ex}} = 260 \text{ nm}$).

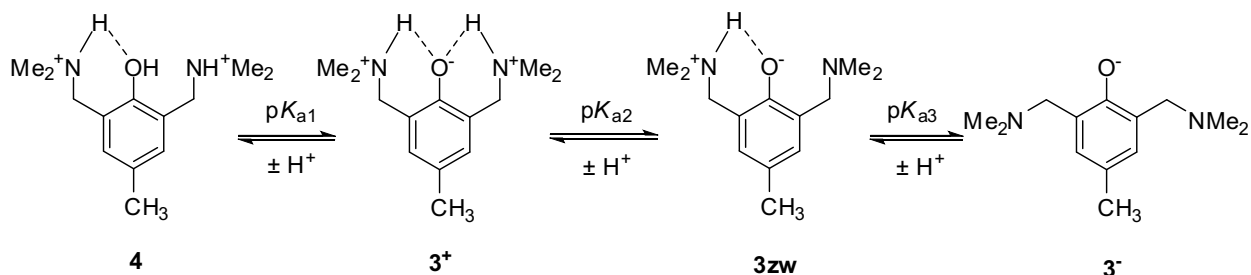
^c Fluorescence quantum yields measured by use of anisole in cyclohexane as a reference ($\Phi_f = 0.29$).⁴⁸

Addition of protic solvent (H₂O) to CH₃CN solutions of **1-4** changed their photophysical properties. When the addition of H₂O did not exceed the concentration of 2 M, the fluorescence

of **2** and **4** was quenched, but increased fluorescence was observed for **1** and **3** (Figs S3, S6, S9, S12 in the Supporting Information). The increase of fluorescence for **1** and **3** by addition of H₂O is due to partial blocking of the efficient non-radiative deactivation pathway from S₁ by ESIPT. Namely, addition of non-buffered H₂O induced protonation of the basic amine nitrogens and formation of **2** and **4**, so that these molecules do not bear a basic center (Schemes 3 and 4). On the contrary, quenching of fluorescence for **2** and **4** by addition of H₂O indicates operation of an additional non-radiative deactivation channel, presumably ESPT to solvent. CH₃CN cannot mediate deprotonation of the phenol in S₁, so presence of a protic solvent (H₂O) is required to enable ESPT.^{49,50} In particular, fluorescence spectrum for **4** in CH₃CN-H₂O exhibit a strong band at 370 nm (Fig. 1 bottom) attributed to the fluorescence of phenolate (in **3**⁺ or **3zw**).



Scheme 3. Protonation equilibria for **2**.



Scheme 4. Protonation equilibria for **4**.

Acid-base properties of **2** and **4**

Acid-base properties were investigated for **2** and **4** by UV-vis pH titrations. The titrations were performed in H₂O in the absence of an ionic buffer by addition of small amounts of NaOH or HCl to adjust the pH. The spectra were processed by multivariate nonlinear regression analysis using the SPECFIT software^{51,52,53} to reveal the p*K*_a values (Table 2).

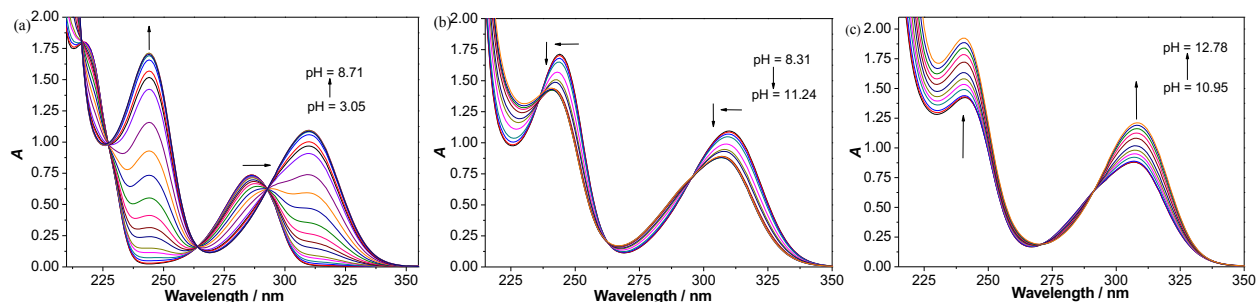
The increase of pH for the aqueous solution of **2** in the range 6-10 induced significant UV-vis spectral changes (Fig. S13-S14 in the Supporting Information). The band at ≈286 nm disappeared with concomitant formation of a new bathochromically shifted band at ≈302 nm. The spectral change is in agreement with the formation of phenolate **1zw** (Scheme 3) where bathochromic shift is due to a larger stabilization of S₁ than S₀ by deprotonation. The p*K*_a value for the equilibrium between **2** and **1zw** is lower than for the parent *p*-cresol (p*K*_a = 10.2)⁵⁴ owing to a stabilization of the negative charge in **1zw** by intramolecular H-bond. However, some influence to the p*K*_a value may be imposed by the non-constant ionic strength of the solution at different pH values. Further increase of pH in the range 10-12 induced deprotonation of the amine moiety (see Fig. S15 in the Supporting Information for the distribution of species with pH). Due to the H-bond between the amine NH and the phenolate O⁻ at the chromophore, the deprotonation resulted in the spectral changes.

Table 2. p*K*_a values for **2** and **4** at 25 °C in aqueous solution.^a

Compound	2	4
p <i>K</i> _{a1}	8.46 ± 0.01	5.87 ± 0.01
p <i>K</i> _{a2}	11.15 ± 0.01	10.00 ± 0.02
p <i>K</i> _{a3}	–	12.31 ± 0.02

^a The titration was conducted in aqueous solution without ionic buffer. p*K*_{a1} corresponds to the first equilibrium in Schemes 3 and 4, while p*K*_{a2} and p*K*_{a3} correspond to the subsequent equilibria.

The UV-vis spectra for **4** at different pH values are shown in Fig. 2. The titration gave rise to three distinctive pH regions with different spectral responses. In the pH region between 3 and 8, the most pronounced spectral changes were observed, due to the deprotonation of the phenolic OH. In contrast to low acidity of phenols ($pK_a = 9.89-9.91$),⁴¹ pK_{a1} of **4** is significantly lower (Table 2) due to the stabilization of phenolate in **3⁺** by two intramolecular H-bonds with the ammonium ion and compensation of the negative charge by two positive charges (Scheme 4). A similar influence to the acidity has been reported for phenols substituted with *o*-amide groups.⁵⁵ The second deprotonation equilibrium is observed in the pH region between 8.3 and 11, and marked by a decrease of the phenolate absorptivity at ≈ 308 nm. The low pK_{a2} value corresponding to the first amine deprotonation is due to a high acidity of this ammonium ion owing to H-bonds with phenolate in **3⁺**. Breaking of the H-bond with the chromophore gives rise to the observed spectral changes. The pK_a for the second amine deprotonation is significantly higher. It is more difficult to remove a proton from neutral molecule **3zw** and form anion **3⁻** because it leads to breaking of the last intramolecular hydrogen bond (see Fig. S16 in the Supporting Information for the distribution of species with pH).



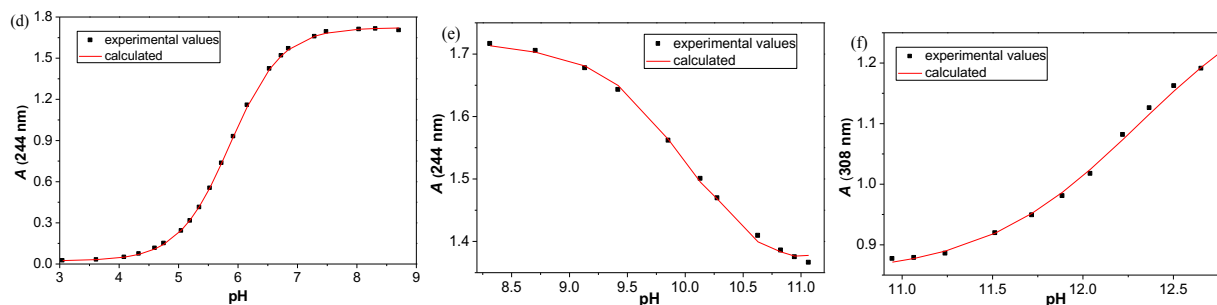


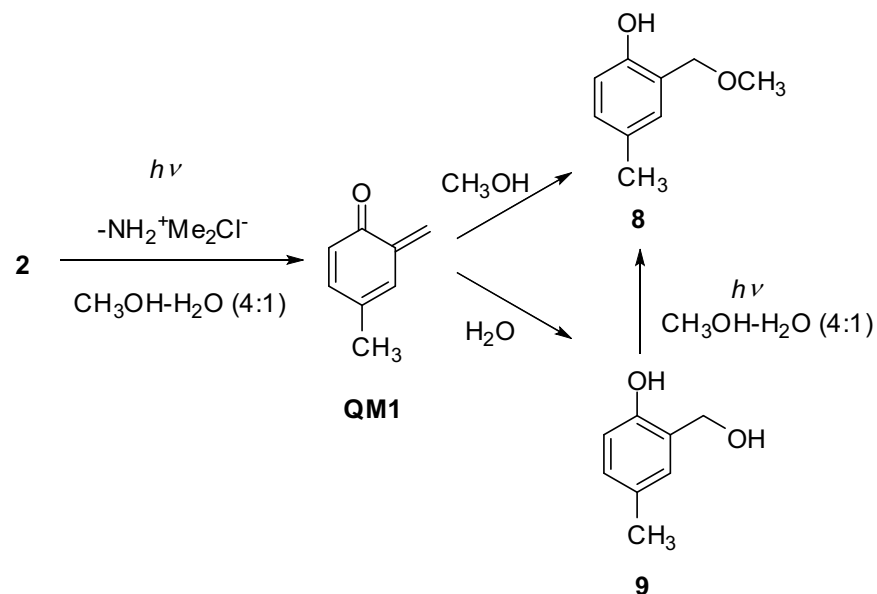
Figure 2. Absorption spectra of **4** ($c = 2.66 \times 10^{-4}$ M) in H₂O at different pH values a) from 3.05 to 8.71, b) from 8.31 to 11.24, c) from 10.95 to 12.78, and dependence of the absorbance at 244 nm (d and e) and at 308 nm (f), corresponding to a-c, respectively. The calculated values (—) were obtained by nonlinear regression analysis of the experimental values (▪) using the SPECFIT software. The titration was performed at 25 °C from acidic solution (HCl) by addition of NaOH. The spectra were corrected for dilutions.

Measurements to construct a Förster cycle were performed to show that S₁ of **1-4** exhibits enhanced acidity despite the limitations in using this method.⁴² Of importance for this work is the trend in the pK_a^* values and not in the absolute value obtained. The difference in the emission maxima of phenol and phenolate seen in the spectra of **4** in aqueous CH₃CN (eq. S2 in the Supporting Information) gave a ΔpK_a of 8.2. Fluorescence titrations were performed to reveal pK_a^* values, but due to the low fluorescence intensity we were not able to process the data with satisfactory accuracy (see Figs S17 and S18). Nevertheless, the titrations indicated decrease of pK_a values upon excitation for both **2** and **4**, in agreement with the Förster cycle analysis.

Photochemical reactivity

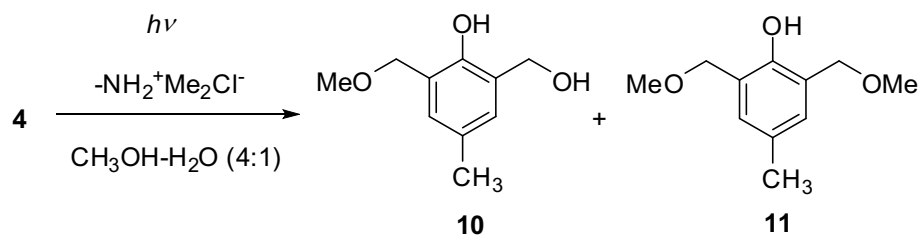
Based on literature precedent,^{8,56} it is expected that irradiation of **1-4** in CH₃OH-H₂O gives rise to photomethanolysis products *via* QM intermediates. Preparative irradiations of **2** and **4** were conducted by irradiating CH₃OH-H₂O (4:1) solutions at 300 nm and by analyzing the

composition of the solutions by HPLC. Methanolysis of **2** run to the conversion of 80% gave methyl ether **8**,⁵⁷ with a yield of 77%. An additional product, presumably alcohol **9**, was detected by HPLC but was not isolated due to the small quantities formed. Preferable formation of **8** is logical due to a better nucleophilicity of CH₃OH compared to H₂O. In addition, alcohol **9** under the same reaction conditions undergoes methanolysis and gives **8**, albeit with lower quantum efficiency (Scheme 5).²⁷



Scheme 5. Photomethanolysis of **2**.

Photomethanolysis of **4** conducted in CH₃OH-H₂O (4:1) to the conversion of 100% gave quantitatively **10**, which was isolated and characterized by NMR. The shorter irradiation of **4** until the conversion was 50% and separation of the mixture by HPLC gave **10** (20%, isolated yield) and **11**⁵⁸ (7%, isolated yield, Scheme 6). Irradiation of **1** and **3** gave the same products as **2** and **4**, respectively.



Scheme 6. Photomethanolysis of **4**.

As described above, presence of H₂O changes the photophysical properties of **1-4**. Therefore, we conducted photomethanolysis of **1** and **2** in CH₃OH at different H₂O concentrations where solutions were irradiated simultaneously and the progress of the reaction was monitored by HPLC (Figs S19-S20 in the Supporting Information). The solutions compared had the same concentrations of compound and the absorbance at the excitation wavelength was above 2 ensuring that all photons were absorbed. Addition of H₂O did not affect the photolysis of **1** with 85% of **8** being formed after 15 min of irradiation in the absence and presence of H₂O. In contrast, the photolysis of **2** was dependent on the water concentration where in neat CH₃OH after 15 min irradiation gave 6% of **8**, while in the presence of 10% H₂O 15% of **8** was formed. No influence of H₂O concentration on the efficiency of photomethanolysis of **1** is due to an efficient ES IPT which is coupled with deamination and does not require a proton accepting solvent for the reaction to occur. On the contrary, for the deamination of salt **2**, H₂O is required for the deprotonation of phenol. It is known that phenol deprotonates faster from S₁ to H₂O-clusters than to CH₃OH.^{59,60,61,62}

Influence of pH on the photochemistry of **2** (Fig. 3) was investigated by conducting photohydrolysis reaction at different pHs. The pH values used were 1.0, 5.3, 9.8 and 14, corresponding to the highest concentrations of species **2**, **1zw** and **1⁻** (Scheme 3 and Fig. S15 in the Supporting Information). The highest efficiency was observed at pH 9.8 demonstrating that

the most reactive species in the photohydrolysis is the zwitterion. Photohydrolysis of salt **2** is four times less efficient than **1zw**, whereas phenolate 1^- is the least reactive, with the efficiency ten times lower than for **1zw**. A similar photohydrolysis experiment at three pH values was conducted with **5** (Fig S21 in the Supporting Information). The irradiation gave compound **12**⁶³ that was isolated and characterized by NMR. It is interesting to note that photohydrolysis of **5** and **2** in acidic conditions wherein the amine and phenol are protonated proceeds with approximately similar efficiency. However, when phenol is in the zwitterionic form **1zw** is much more reactive than methoxy derivative **5**.

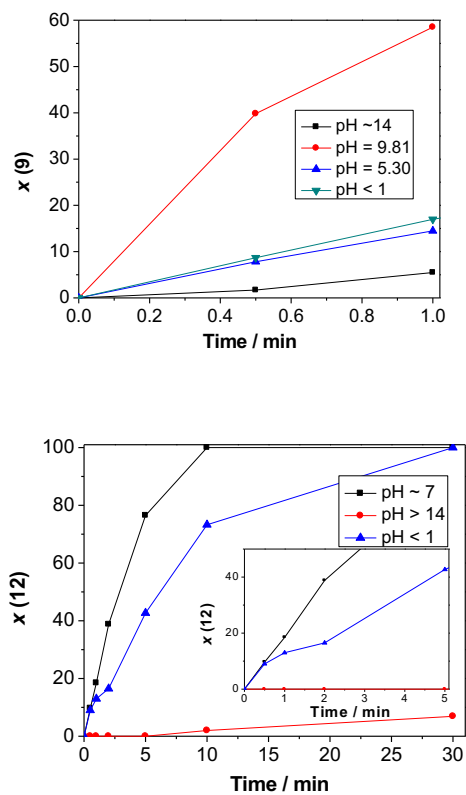
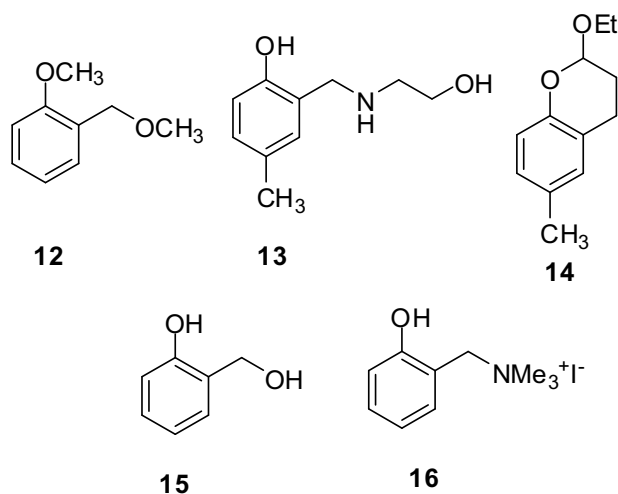


Figure 3. Dependence of the photohydrolysis efficiency on pH of **2** (top), and **5** (bottom, inset: 5 min. expansion).

To show that **QM1** is an intermediate in the photochemistry of **2**, irradiation was performed in CH_3CN solution in the presence of ethanolamine, an ubiquitous quencher of QMs.^{4,31,64,65,66} However, after the irradiation adduct **13** was not detected. Since ethanolamine is a base, the finding is in accord with less efficient photohydrolysis in basic conditions at $\text{pH} > 12$. The irradiation of **2** in neat CH_3CN was also performed in the presence of ethyl vinyl ether which is known to react with QMs in a Diels-Alder reactions.⁶⁷ The irradiation gave chromane **14**,⁶⁸ isolated in the yield of 42%, clearly indicating the existence of **QM1** as an intermediate during the solvolysis.



The efficiency of the photomethanolysis (Φ_R) for **1-4** was investigated by simultaneous use of three actinometers, ferrioxalate ($\Phi_{254} = 1.25$),^{48,69} KI/KIO_3 ($\Phi_{254} = 0.74$),^{48,70} and valerophenone ($\Phi_{254} = 0.65 \pm 0.03$).^{48,71} The same method was used to determine the Φ_R for **15** and **16** (Table 3). Φ_R for **15** is within the experimental error with the reported value ($\Phi_R = 0.23$),²⁷ whereas for our experimental conditions Φ_R for **16** is much lower than reported ($\Phi_R = 0.98$).⁸ It is interesting to note that methanolysis of alcohol **15** is about two times more efficient than of amine **1**.

Transformation to salts **2** and **16** increases the quantum efficiency by about four times. Bi-functional derivatives **3** and **4** undergo more efficient reactions than the corresponding **1** and **2**.

Table 3. Quantum efficiency for methanolysis (Φ_R) of **1-4**, **15** and **16**.^a

Compound	Φ_R
1	0.11 ± 0.01
2	0.42 ± 0.03
3	0.42 ± 0.05
4	0.91 ± 0.03
15	0.20 ± 0.02^b
16	0.40 ± 0.02^c

^a Measured in neutral CH₃OH-H₂O (4:1) by averaging the values obtained from using three actinometers, ferrioxalate ($\Phi_{254} = 1.25$),^{48,69} KI/KIO₃ ($\Phi_{254} = 0.74$),^{48,70} and valerophenone ($\Phi_{254} = 0.65 \pm 0.03$).^{48,71} The errors correspond to the values obtained from three independent measurements, each with three actinometers.

^b Measured in neutral CH₃OH-H₂O (1:1). The literature value $\Phi_R = 0.23$.²⁷

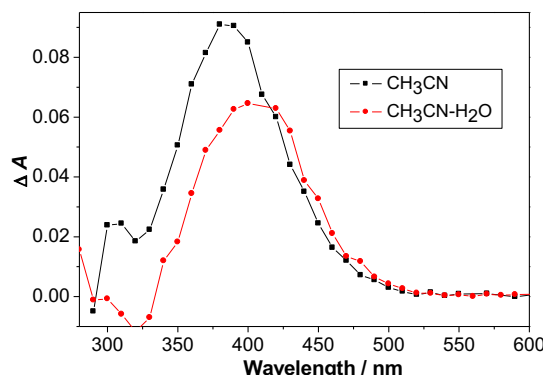
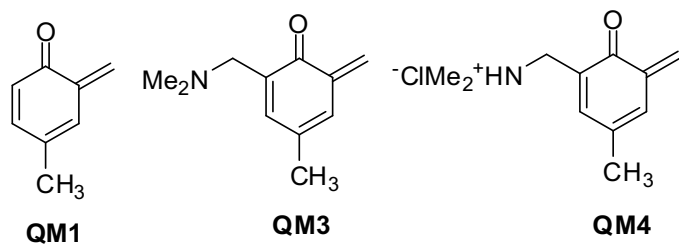
^c Measured in neutral CH₃OH-H₂O (1:1). The literature value $\Phi_R = 0.98.8$ The difference is probably due to different measurement conditions.

The potential thermal reactivity of **1-4** and **16** (10^{-3} M) in methanolysis was probed by the analysis of the CH₃OH-H₂O (1:1) solutions at different pHs (1, 7 and 14) by HPLC. The analysis revealed that **1-4** were stable over 15 days, whereas **16** underwent methanolysis with the conversion of 23% over 15 days.

Laser Flash Photolysis (LFP)

LFP measurements with excitation at 266 nm for solutions in CH₃CN and CH₃CN-H₂O (1:1) were performed for **1-4**, to probe for the formation of QMs. In both solvents QMs are expected to be formed, but ESPT to solvent is only possible in CH₃CN-H₂O. The transient absorption

spectra of **1-4** in both CH₃CN and CH₃CN-H₂O (1:1) solutions are characterized by an absorption band with a maximum at ≈ 400 nm. The transients are formed within the 10 ns laser pulse and therefore the kinetics for formation of the transients could not be resolved. For **1** and **2** the spectra are shown in figure 4 and for **4** in figure 5 (for other spectra as well as quenching plots see. Figs. S22- S40 in the Supporting Information). The transients decayed to the baseline with unimolecular kinetics, except for **4** in CH₃CN-H₂O where the decay was fit to a sum of two exponentials (see below). The presence of O₂ did not affect the efficiency of the formation of the transients neither did it affect the decay rates, in agreement with the formation of transients from the singlet excited state and the formation of transients that do not react with O₂. The transients were assigned to **QM1**, **QM3** and **QM4** based on precedent literature with respect to the position of transient absorption maximum, the decay kinetics,^{8-26,27} and the lack of influence of O₂ on the decay kinetics.



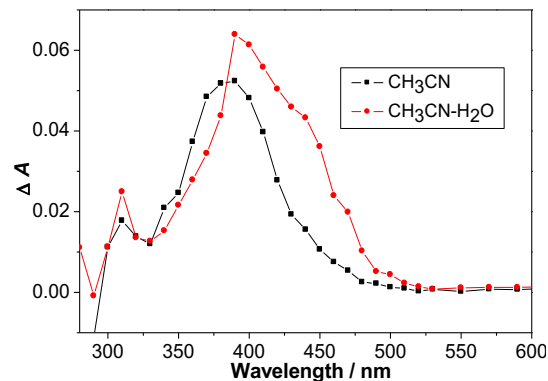


Figure 4. Transient absorption spectra in O₂ purged and optically matched ($A_{355} \approx 0.31$) solutions for **1** (top, delay = 8 μ s) and **2** (bottom, delay = 10 μ s) in CH₃CN and in CH₃CN-H₂O. The lifetimes of the transients are compiled in Table 4.

Table 4. Lifetimes of **QM1-QM4** measured by LFP in O₂-purged CH₃CN or CH₃CN-H₂O.^a

Compound	τ (CH ₃ CN) / ms	τ (CH ₃ CN-H ₂ O) / ms
QM1	5 ± 1 ^b	2.5 ± 0.2 ^b
	200 ± 20 ^c	105 ± 10 ^c
QM3	2.0 ± 0.2	3 ± 1
QM4	0.12 ± 0.01	14 ± 2 and 135 ± 5 ^d

^a The LFP system was adapted to measure ms lifetimes.⁷²

^b Measured for **1**.

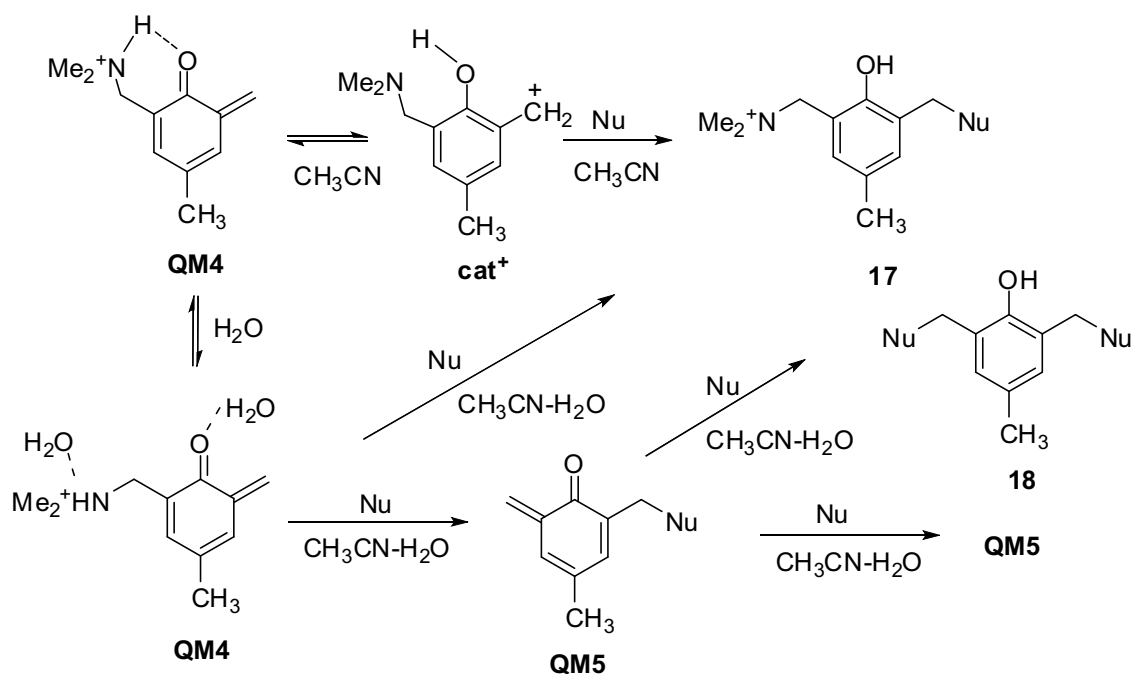
^c Measured for **2**.

^d The decay kinetics were fit to sum of two exponentials.

The deamination of both cresols **1** and **2** gives rise to the same **QM1**. Cresol **1** bears a nucleophilic amine which is not present in salt **2**. As a consequence, **QM1** formed from **1** has a 40 times shorter lifetime than from **2** due to reaction of **QM1** with dimethyl amine which quenches **QM1**. The difference in lifetimes for **QM1** corresponds to the quenching rate constant with dimethylamine of approximately $4 \times 10^6 \text{ M}^{-1}\text{s}^{-1}$ (assuming 10% conversion of **1** to **QM1** by laser pulse at the concentration of **1** at $5 \times 10^{-4} \text{ M}$). Addition of H₂O to the CH₃CN solution changed the efficiency of the transient formation, judged from the intensity of the transient

absorbance immediately after the laser pulse when solutions with the same absorbance at the excitation wavelength are compared. Thus, **QM1** is formed 1.5 more efficiently from **1** in aprotic solution, whereas for salt **2** the reaction is 1.2 more efficient in the presence of H₂O. This result is in agreement with the fluorescence measurements and influence of H₂O on the methanolysis efficiency (see above). All these results clearly indicate that protic solvent increases the rate of deamination of the salts, whereas it decreases the rate for the amines. The decay kinetics of **QM1-QM3** is slower in CH₃CN than in the presence of H₂O, which is in agreement with the reaction of QMs with H₂O.^{26,27,28,31,64,65,66,73,74,75}

Contrary to **QM1** and **QM3**, **QM4** exhibits about 100 times shorter lifetime in CH₃CN than in aqueous solution (Figure 5). This shorter lifetime of **QM4** in CH₃CN is probably due to intramolecular protonation of the carbonyl oxygen by the ammonium salt along the intramolecular H-bond, rendering **QM4** (or the resulting **cat⁺**, Scheme 7) more reactive with nucleophiles. Acid catalysis in the hydration reactions of QMs has been demonstrated.^{26,73,74,75,76,77} Addition of H₂O to the CH₃CN solution probably disrupts the intramolecular H-bond in **QM4** leading to the less efficient protonation of the QM carbonyl and longer lifetime. Interestingly, the decay of **QM4** in aqueous solution was fit to sum of two exponentials (Fig 5. bottom). This finding was explained by two reactions of **QM4**, one leading to new **QM5**, and the other to adduct **17** (Scheme 7). Since the spectra of **QM4** and **QM5** overlap, biexponential decay of the transient absorption was observed. The short decay time probably corresponds to **QM4**, and the long one to **QM5**. Such a biexponential decay was not observed for **QM3** since the amine is a worse leaving group compared to the ammonium salt. That is, upon attack of nucleophile to **QM3**, only adducts can be formed, and not a QM as shown in Scheme 7 for the protonated derivative **QM4**.



Scheme 7. Reactions of **QM4**.

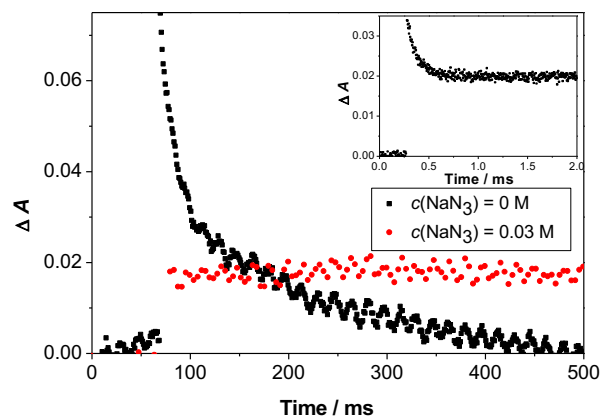
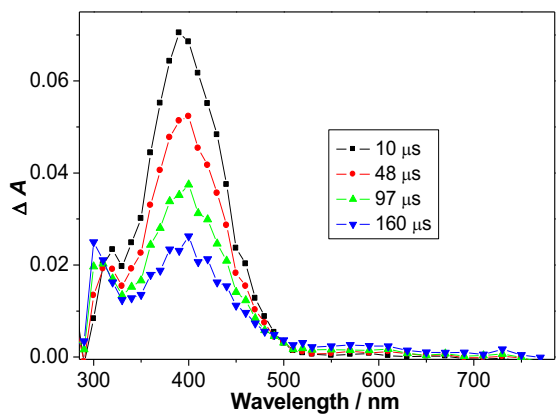


Figure 5. Top: Transient absorption spectra of **4** in O₂-purged CH₃CN. Bottom: Decay of the transient absorption at 420 nm in CH₃CN-H₂O (1:1) solution of **4** ($c = 6 \times 10^{-4}$ M) without quencher and in the presence of NaN₃ (0.03 M) (Inset: decay at 420 nm in the presence of 0.03 M NaN₃ at short timescale).

Additional evidence for the assignment of the observed transients to QMs was obtained through quenching studies. The quenching was conducted with nucleophiles CH₃OH, ethanolamine, NaN₃ and ethyl vinyl ether (EVE) that reacts with QMs in a Diels-Alder reaction (Figs S22-S40 in the Supporting Information). Some of the quenching rate constants are only approximate values due to imprecise kinetic measurements at long timescales (Table 5). All values are in agreement with the precedent in the literature.^{48,76,77} In the quenching experiment of **QM4** it is interesting that addition of NaN₃ quenches only the short decay for which only an estimate could be provided of $(1-10) \times 10^6 \text{ M}^{-1}\text{s}^{-1}$ due to poor quality of quenching plot, whereas the long decay component ($\tau = 135 \pm 5$ ms) become longer-lived ($\tau > 10$ s). This finding was explained by reaction of **QM5** with N₃⁻ in which N₃⁻ is also the leaving group (Scheme 7). The reaction does not give rise to a new product since **QM5** is regenerated, which leads to the observed long-lived transient absorption. However, formation of **18** is eventually expected leading to the decay of this transient.

Table 5. Quenching rate constants ($k_q / \text{M}^{-1} \text{s}^{-1}$) obtained by LFP.

Quencher	QM1	QM3	QM4
CH ₃ OH ^c	430 ± 40 ^a _d	–	–
Ethanolamine ^e	(9.7 ± 0.2) × 10 ⁴ ^a (1.0 ± 0.2) × 10 ⁵ ^b	(6.8 ± 0.4) × 10 ⁴	(5.5 ± 0.2) × 10 ⁴ ^f
NaN ₃ ^e	(5.0 ± 0.1) × 10 ⁶ ^a (4.9 ± 0.3) × 10 ⁶ ^b	(3.6 ± 0.1) × 10 ⁶	(1-10) × 10 ⁶ ^g
EVE ^e	600-800 ^a _d	700-1300	–

^a The transient formed from **1**.

^b The transient formed from **2**.

^c Measured in CH₃CN.

^d The transient was too long-lived for the accurate measurement of the quenching rate constant.

^e Measured in CH₃CN-H₂O (1:1).

^f Measured in CH₃CN-H₂O (1:1). The decay becomes single exponential in the presence of a base.

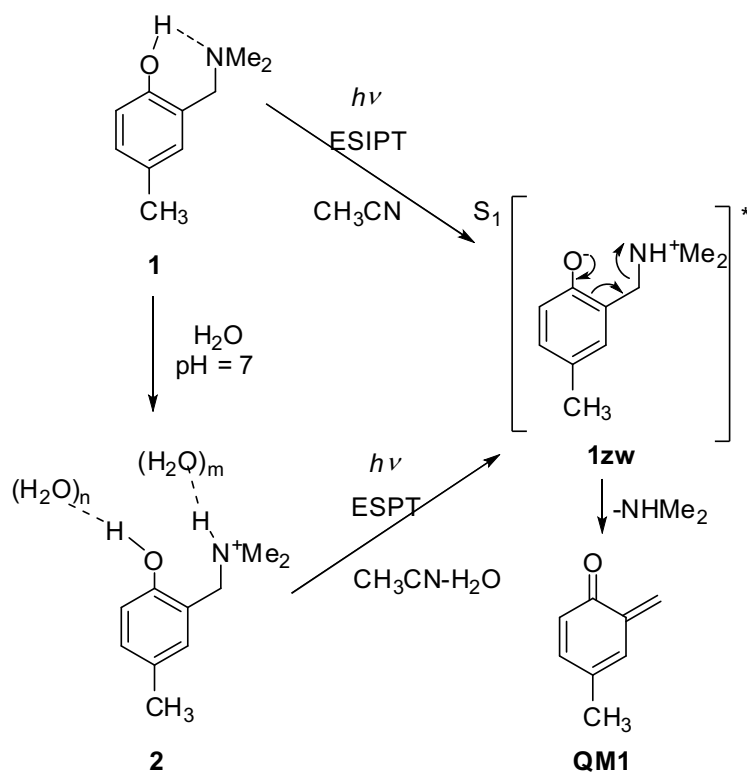
^g The short decay component is quenched (only order of magnitude estimate was possible because of poor quality of quenching plot, Fig. S39 in the Supporting Information), whereas the slow-decaying transient becomes long-lived with the lifetime > 10s.

Discussion

The results show unequivocally that the mechanism for the photodeamination of amines **1** and **3** can be different from the photodeamination of salts **2** and **4** depending on the solvent system, showing that the presence of a basic site in **1** and **3** leads to efficient ES IPT while for the salts that do not have this basic site the proton transfer has to occur to the solvent. Such a difference has a direct impact on the photodeamination reactivity in hydrophobic sites of biological systems where the availability of water may be limited.

The different reactivity will be illustrated for amine **1** and the corresponding salt **2**. On excitation of **1** in aprotic solvent (CH₃CN), adiabatic ES IPT takes place along the intramolecular H-bond and gives zwitterion **1zw**, which was detected by fluorescence spectroscopy as a species that emits at a longer wavelength. Due to efficient ES IPT, singlet excited state lifetime of **1** is expected to be short and the fluorescence quantum yield is low. Formation of **1zw** in S₁ is followed by deamination, also occurring from S₁. Namely, **1zw** is antiaromatic in S₁,^{78,79} leading to the formation of the more stable **QM1** (Scheme 8). In aqueous solution at pH 7, the amine is protonated (Table 2) and the dominant species is cation **2**. Therefore, ES IPT cannot take place. Instead, ES PT to proton-accepting solvent upon excitation gives **1zw**, which is the reactive

species in the photodeamination. The quantum yield for the formation of **QM1** in a protic solvent is 1.5 lower than in neat CH₃CN, as demonstrated by LFP, suggesting that ES IPT is more efficient than ESPT to solvent, both of which are coupled with deamination. **QM1** ultimately gives adducts with nucleophiles or undergoes Diels-Alder reaction with dienophiles.

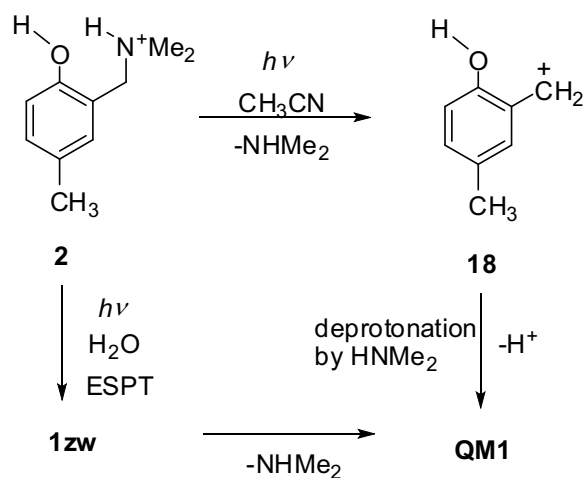


Scheme 8. Mechanism of QM1 formation from **1**.

ESPT to CH₃CN cannot take place due to its weak proton accepting properties.^{42,43,49,50,59,60,61,62} Moreover, ES IPT is not possible in salt **2** that does not contain a basic site. Since photosolvolysis of ether **5** takes place, but cannot involve formation of QMs, it is highly conceivable that photosolvolysis of **5** and deamination of **2** in aprotic solvent proceed *via* a similar mechanism. Most probably, excitation of **2** to S₁ in aprotic solvent leads first to the cleavage of the ammonium giving cation **18** (Scheme 9), followed by the deprotonation in the attack of

dimethylamine giving **QM1**. We have no spectral evidence for the formation of cation **18** and at this point it remains undetected.

The efficiency of the reaction is related to the prototropic form of the reactant molecule. When **2** is dissolved in aqueous solvent at pH 7, the photodeamination takes place more efficiently due to proton transfer to the solvent and follows the same mechanism as discussed for **1**. Increase of the pH leads to the formation of **1zw** that further increases the efficiency of photodeamination (Scheme 9). However, above pH 11 the photodeamination is the least efficient. At such a high pH, anion **1⁻** is the dominant species, which is not very reactive since dimethylamine is a poor leaving group.



Scheme 9. Mechanism of QM1 formation from **2**.

The mechanism of QM formation from bifunctional derivatives **3** and **4** follows the same mechanism in aprotic solvent, as discussed for **1** and **2**. However, in aqueous solution one more acid-base equilibrium exists. Thus, in aqueous solution at pH 7, the diamine is present in its monocationic form **3⁺** which is the most reactive form in the deamination reaction. Therefore, the

deamination takes place very efficiently, as judged from the methanolysis quantum yield for **4** ($\Phi_R = 0.91$). Moreover, an additional electron-donor group in **QM3** and electron-acceptor in **QM4**, change the reactivity of **QM4** compared to **QM1**, as demonstrated in the reaction with azide, and in line with precedent in the literature.⁵⁶ Particularly interesting is the reactivity of **QM4** which bears very good leaving group. Thus, attack of nucleophiles gives rise to the new **QM5**, or to adducts **17**. This finding is particularly important for the application of **QM4** in biological systems for the formation of thermodynamically most stable DNA cross-links. Reversible alkylation of DNA by QMs and "immortalization of QM" by DNA as a nucleophile has been postulated,^{16,80,81,82} wherein initial formation of DNA alkylation products formed under kinetic control follows repeated capture and release of the QM until thermodynamic most stable products are formed. However, to the best of our knowledge, a spectral evidence for the competing reactions of bifunctional QMs has not yet been provided. Our results cannot completely rule out other mechanistic scenarios that lead to solvolysis products and do not involving QMs. However, if they take place they should be very inefficient.

Conclusion

Cresol derivatives **1-4** were synthesized and their acid-base properties, photophysics and photochemical reactivity in photodeamination reactions investigated. On excitation to S_1 the cresols become more acidic. Therefore, amine derivatives **1** and **3** in aprotic solvent in S_1 undergo ES IPT giving zwitterions **1zw** and **3zw**, which subsequently in the photodeamination reaction give **QM1** and **QM3**, respectively. Salts **2** and **4** cannot deactivate by ES IPT. However, photodeamination from these salts takes place wherein the ammonium group is presumably cleaved first to give undetected benzyl cation, and subsequently deprotonation gives **QM1** and

QM4. Although **1** and **2** give the same **QM1**, the lifetime of the transient is different as well as the overall efficiency in the photosolvolysis. **QM1** exhibits shorter lifetime when formed from **1** (τ in CH₃CN = 5 ms) then from **2** (τ in CH₃CN = 200 ms) due to the reaction with eliminated dimethylamine. In aqueous solvent, deamination depends largely on the prototropic form of the molecule. The most efficient deamination takes place when the amine is in the zwitterionic form (pH 9-11) and the diamine in the monocationic form (pH 7-9). **QM1**, **QM3** and **QM4** were detected by LFP ($\lambda_{\text{max}} = 400$ nm, $\tau = 0.1$ -200 ms) and the rate constants of their reactions with nucleophiles were measured. Bifunctional **QM4** with a good leaving group undergoes two types of reactions with nucleophiles, giving adducts or new QMs. The result is of significant importance for biological systems, where bifunctional QMs are used in the DNA cross-linking. Unrevealing differences in reactivity of salts and amines studied in this work is important in the use of QMs for alkylation of proteins wherein hydrophobic microenvironment or proximity of acidic or basic amino acid residues can significantly alter kinetics of their formation and decay. Moreover, we have shown herein that deamination in aqueous solution can be controlled by pH which could have some implications in biology, for example in controlled drug delivery. In principle, instead of methyl groups on the amine, salt **2** can be substituted with a drug, such as amantadine or memantine, that would efficiently undergo photodeamination and drug release, only in the pH region 8.5-10.5.

Experimental section

General

¹H and ¹³C NMR spectra were recorded at 300 or 600 MHz at rt using TMS as a reference and chemical shifts were reported in ppm. Melting points were determined using a Mikroheiztisch

apparatus and were not corrected. IR spectra were recorded on a spectrophotometer in KBr and the characteristic peak values were given in cm^{-1} . HRMS were obtained on a MALDI TOF/TOF instrument. Irradiation experiments were performed in a reactor equipped with 11 lamps with the output at 300 nm or a reactor equipped with 8 lamps. During the irradiations, the irradiated solutions were continuously purged with Ar and cooled by a tap-water finger-condenser. Solvents for irradiations were of HPLC purity. Chemicals were purchased from the usual commercial sources and were used as received. Solvents for chromatographic separations were used as they are delivered from supplier (p.a. or HPLC grade) or purified by distillation (CH_2Cl_2).

2-[(*N,N*-dimethylamino)methyl]-4-methylphenol (1)

In a round bottom flask (50 mL) *p*-cresol (163 mg, 1.51 mmol) and anhydrous K_2CO_3 (313 mg, 2.26 mmol) were suspended in CH_2Cl_2 (10 mL). *N,N*-dimethylmethyleiminium chloride (142 mg, 1.52 mmol) was added and the reaction mixture was stirred at rt for 16 h. The next day, the reaction mixture was filtered and the solid was washed with ethyl acetate. The solvent was removed on a rotary evaporator to furnish crude oily product, which was purified on a column of alumina (act. IV) using CH_2Cl_2 as eluent to afford 222 mg (93 %) of pure **1** in a form of colorless viscous oil. Characterization of **1** is in accord with the precedent literature.⁸³ ^1H NMR (CDCl_3 , 300 MHz) δ /ppm 6.96 (dd, 1H, $J = 8.1, 1.2$ Hz), 6.76 (d, 1H, $J = 1.2$ Hz), 6.72 (d, 1H, $J = 8.1$ Hz), 3.59 (s, 2H), 2.31 (s, 6H), 2.23 (s, 3H); ^{13}C NMR (CDCl_3 , 75 MHz) δ /ppm 155.5, 128.9, 128.7, 127.8, 121.5, 115.6, 62.8, 44.4, 20.3.

2-[(*N,N*-dimethylamino)methyl]-4-methylphenol hydrochloride (2)

To the solution of amine **1** (200 mg) in CH₂Cl₂-Et₂O (1:1, 5 mL), a saturated solution of HCl in Et₂O was added whereupon white precipitate was formed. The precipitate was filtered and washed with Et₂O (3×10 mL). Drying in a desiccator over KOH afforded 222 mg (93 %) of **2** in the form of colorless crystals: ¹H NMR (DMSO-*d*₆, 300 MHz) δ/ppm 10.1 (s, 1H), 10.0 (br s, 1H), 7.23 (d, 1H, *J* = 1.8 Hz), 7.07 (dd, 1H, *J* = 8.2, 1.8 Hz), 6.90 (d, 1H, *J* = 8.2 Hz), 4.15 (d, 2H, *J* = 4.9 Hz), 2.69 (d, 6H, *J* = 4.6 Hz), 2.22 (s, 3H); ¹³C NMR (DMSO-*d*₆, 150 MHz) δ/ppm 154.2, 132.9, 131.4, 127.6, 116.1, 115.5, 54.6, 41.7, 19.9.

2,6-Bis[(*N,N*-dimethylamino)methyl]-4-methylphenol (3**)**

In a round bottom flask (50 mL) equipped with a condenser, *p*-cresol (2.34 g, 21.6 mmol), dimethylamine (40 % aq, 8.2 mL, 64.8 mmol) and formalin (37 % aq, 4.2 mL, 56 mmol) were mixed and heated at the temperature of reflux over 2 h. After cooling to rt, solid NaCl was added whereupon the layers were separated. The upper organic layer was dried with anhydrous Na₂SO₄ and the solid was filtered off. The crude product was purified on a column of alumina (act. IV/V) using CH₂Cl₂ as eluent to afford 4.19 g (87 %, lit.⁸⁴ 39 %) of colorless oil. Characterization of **3** is in accord with the precedent literature.⁸⁴ ¹H NMR (CDCl₃, 300 MHz) δ/ppm 6.83 (s, 2H), 3.50 (s, 4H), 2.29 (s, 12H), 2.23 (s, 3H); ¹³C NMR (CDCl₃, 300 MHz): δ/ppm 154.1 (s), 129.1 (d), 127.1 (s), 122.9 (s), 60.3 (t), 44.7 (q), 20.3 (q).

2,6-Bis[(*N,N*-dimethylamino)methyl]-4-methylphenol hydrochloride (4**)**

To the solution of amine **3** (50 mg) in CH₂Cl₂-Et₂O (1:1, 5 mL), a saturated solution of HCl in Et₂O was added whereupon white precipitate was formed. The precipitate was filtered through a sinter and washed with Et₂O (3×10 mL). The crude product was purified by crystallization from

CH₃OH-Et₂O at 4 °C. Pure product **4** (55 mg, 82 %) was obtained in the form of colorless crystals. ¹H NMR (DMSO-*d*₆, 600 MHz) δ/ppm 7.41 (s, 2H), 4.34 (s, 4H), 2.72 (s, 12H), 2.25 (s, 3H); ¹³CNMR (DMSO-*d*₆, 150 MHz) δ/ppm 153.3, 135.1, 129.1, 119.5, 54.5, 41.6, 19.9.

2-Methoxybenzaldehyde (6)

Salicylaldehyde (1.2 g, 10 mmol), Na₂CO₃ (1.3 g, 12 mmol), THF (60 mL) and MeOH (15 mL) were mixed in a two-necked round flask (100 mL) equipped with a reflux condenser. MeI (1.9 mL, 30 mmol) was added dropwise and the resulting suspension was refluxed overnight. The reaction mixture was poured on water (200 mL) and extracted with CH₂Cl₂ (3×30 mL). Combined organic extracts were dried on MgSO₄, filtered and the solvent was removed on a rotary evaporator to obtain 1.29 g (95%) of product in the form of yellowish oil. The product was used in the next step without further purification. NMR spectra of **6** is in accord with the known spectra.⁴⁰ ¹H NMR (CDCl₃, 600 MHz) δ/ppm 10.5 (s, 1H), 7.83 (dd, 1H, *J* = 7.5 and 1.7 Hz), 7.57-7.53 (m, 1H), 7.03 (t, 1H, *J* = 7.5 Hz), 6.99 (d, 1H, *J* = 8.4 Hz), 3.93 (s, 3H); ¹³C NMR (CDCl₃, 75 MHz) δ/ppm 189.7 (d), 161.7 (s), 135.8 (d), 128.5 (d), 124.8 (s), 120.6 (d), 111.5 (d), 55.5 (q).

2-(*N,N*-dimethylamino)methyl-1-methoxybenzene hydrochloride (5)

Compound **6** (272 mg, 2 mmol) and 40% aqueous dimethylamine (1 mL, 7.9 mmol) were dissolved in abs. methanol (20 mL) in a round-bottomed flask and stirred vigorously overnight. The *in situ* formed Schiff base underwent reductive amination under a hydrogen atmosphere (balloon, 1 atm) and PtO₂ catalyst (20 mg, 0.09 mmol). The mixture was then filtered, and the solvent removed on a rotary evaporator to afford a brown oil. The product was purified on a

short column of silica gel using hexane/ethyl acetate (9:1) as eluent to afford 39 mg (55%) of yellow oil (**7**), which was immediately converted to the corresponding hydrochloride salt **5** by HCl in MeOH. The salt was recrystallized three times from acetonitrile/ether (7:3) to obtain 250 mg (62%) of the pure product in a form of white solid. m.p. 147-148 °C (lit.³⁹ 149 °C). ¹H NMR (D₂O, 300 MHz) δ /ppm 7.60-7.52 (m, 1H), 7.41 (dd, 1H, $J = 7.5, 1.6$ Hz), 7.16 (d, 1H, $J = 8.3$ Hz), 7.10 (t, 1H, $J = 7.5$ Hz), 4.33 (s, 2H), 3.93 (s, 3H), 2.86 (s, 6H); ¹³C NMR (D₂O, 75 MHz) δ /ppm 158.6 (s), 133.0(d), 132.8 (d), 121.6 (d), 118.3 (s), 112.0 (d), 58.0 (t), 56.1 (q), 43.1 (q).

Irradiation experiments

4-Methyl-2-methoxymethylphenol (8**)**

A quartz vessel was filled with a solution of **2** (17 mg, 0.084 mmol) in CH₃OH-H₂O (4:1, 50 mL) and the solution was purged with N₂ (20 min), sealed and irradiated in a reactor at 300 nm with 8 lamps over 30 min. After the irradiation, the solvent was removed on a rotary evaporator and the residue purified on a column of silica using CH₂Cl₂ as eluent to afford 10 mg (77 %) of **8** in the form of colorless oil. Characterization of product **8** is in accord with the precedent literature.⁵⁷

¹H NMR (CDCl₃, 600 MHz): δ 7.21 (s, 1H), 7.00 (d, 1H, $J = 8.1$ Hz), 6.81 (br s, 1H), 6.78 (d, 1H, $J = 8.1$ Hz), 4.62 (s, 2H), 3.42 (s, 3H), 2.25 (s, 3H); ¹³C NMR (CDCl₃, 150 MHz): δ 153.8 (s), 129.8 (d), 128.9 (s), 128.6 (d), 121.6 (s), 116.2 (d), 74.1 (t), 58.0 (q), 20.6 (q).

Preparative irradiation of 2,6-Bis[(*N,N*-dimethylamino)methyl]-4-methylphenol hydrochloride (4**)**

A quartz vessel was filled with a solution of **4** (100 mg, 0.34 mmol) in CH₃OH-H₂O (4:1, 100 mL), the solution was purged with Ar (20 min), and irradiated in a reactor at 300 nm with 11 lamps over 20 min. During the irradiation the solution was continuously purged with Ar and cooled with a finger condenser. After the irradiation, the solvent was removed on a rotary evaporator and the residue purified by a preparative HPLC on a C18 column (250×5 mm, 5 μm) and MeOH-H₂O (6:4 + 0.5 % HOAc) eluent to afford pure products **10** and **11** (both as thick colorless oils).

6-Hydroxymethyl-4-methyl-2-methoxymethylphenol (10) 4 mg (7 %); ¹H NMR (CDCl₃, 300 MHz) δ/ppm 6.95 (s, 1H), 6.83 (s, 1H), 4.71 (s, 2H), 4.62 (s, 2H), 3.44 (s, 3H), 2.25 (s, 3H); ¹³C NMR (CDCl₃, 150 MHz) δ/ppm 152.0 (2C, s, d), 128.9 (d), 128.8 (s), 128.1 (d), 127.0 (s), 122.6 (s), 71.7 (t), 62.6 (t), 58.2 (q), 20.3 (q); IR (KBr, cm⁻¹): 3400 (vs), 2921 (s), 2868 (m), 2825 (w), 1719 (w), 1650 (w), 1617 (s), 1484 (vs), 1382 (s), 1228 (s), 1159 (m), 1090 (s), 1032 (w), 867 (m); HRMS (MALDI-TOF) *m/z* [M-H]⁺ calcd for (C₁₀H₁₄O₃) 181.0870, found 181.0867.

4-Methyl-2,6-bis(methoxymethyl)phenol (11) 20 mg (30 %);⁵⁸ ¹H NMR (CDCl₃, 600 MHz) δ/ppm 7.55 (br.s, 1H), 6.92 (s, 2H), 4.56 (s, 4H), 3.43 (s, 6H), 2.25 (s, 3H); ¹³C NMR (CDCl₃, 150 MHz) δ/ppm 151.8 (s), 128.9 (d), 128.6 (s), 123.2 (s), 71.8 (q), 58.1 (q).

1-Methoxy-2-methoxymethylbenzene (12)

A quartz vessel was filled with a solution of **7** (20 mg, 0.1 mmol) in CH₃OH-H₂O (4:1, 35 mL), the solution was purged with N₂ (20 min), sealed and irradiated in a reactor at 300 nm with 8 lamps over 60 min. After the irradiation, the solvent was removed on a rotary evaporator and the

residue purified on a column of silica using CH₂Cl₂ as eluent to afford 11 mg (59 %) of **12** in the form of colorless oil. Characterization of product **12** is in accord with the precedent literature.⁶³

¹H NMR (CDCl₃, 300 MHz) δ /ppm 7.34 (d, 1H, J = 7.4 Hz), 7.30-7.22 (m, 1H), 6.95 (t, 1H, J = 7.4 Hz), 6.87 (d, 1H, J = 8.1 Hz), 4.50 (s, 2H), 3.83 (s, 3H), 3.42 (s, 3H); ¹³C NMR (CDCl₃, 150 MHz) δ /ppm 157.1 (s), 129.0 (d), 128.6 (d), 126.4 (s), 120.3 (d), 110.1 (d), 69.4 (t), 58.2 (q), 55.3 (q).

2-Ethoxy-6-methylchromane (14)

A quartz vessel was filled with a solution of **2** (20 mg, 0.1 mmol) in CH₃CN (20 mL). The solution was purged with Ar (20 min) and ethyl vinyl ether (5 mL, 20.9 mmol) was added. The solution was irradiated in a reactor at 300 nm with 11 lamps over 30 min.

During the irradiation, the solution was continuously purged with Ar and cooled with a finger condenser. After the irradiation, the solvent was removed on a rotary evaporator and the residue purified on a column of silica gel using CH₂Cl₂ as eluent to afford pure product **14** (8 mg, 42%) in the form of colorless oil. Characterization of **14** is in accord with the precedent literature:⁶⁸ ¹H NMR (CDCl₃, 600 MHz) δ /ppm 6.90 (d, 1H, J = 8.1 Hz), 6.86 (s, 1H), 6.72 (d, 1H, J = 8.1 Hz), 5.22 (t, 1H, J = 2.9 Hz), 3.90-3.84 (m, 1H), 3.66-3.60 (m, 1H), 2.97-2.90 (m, 1H), 2.62-2.56 (m, 1H), 2.25 (s, 3H), 2.04-1.99 (m, 1H), 1.96-1.90 (m, 1H), 1.18 (t, 3H, J = 7.1 Hz); ¹³C NMR (CDCl₃, 150 MHz): δ 149.9 (s), 129.6 (s), 129.5 (d), 127.7 (d), 122.2 (s), 116.5 (d), 96.8 (d), 63.4 (t), 26.6 (t), 20.4 (t), 20.3 (q), 15.0 (q).

Measurements of photomethanolysis quantum yields

The quantum yield of the photomethanolysis reaction was determined by use of three actinometers during the same experiment: ferrioxalate ($\Phi_{254} = 1.25$),^{48,69} KI/KIO₃ ($\Phi_{254} = 0.74$),^{48,70} and valerophenone ($\Phi_{254} = 0.65 \pm 0.03$).^{48,71} The measurement of irradiance was described in detail in our previous work,⁸⁵ and the same procedures were employed in this work. The solutions of compounds **1-4** in CH₃OH-H₂O (4:1), **15** and **16** in CH₃OH-H₂O (1:1) were prepared and their concentrations were adjusted to have absorbances of 0.4–0.8 at 254 nm. The solutions were purged with a stream of N₂ (20 min each), and then sealed with a cap. Solution of compounds and actinometers were irradiated in quartz cuvettes (each have same geometry) at the same time with 1 lamp (254 nm). The similar values of irradiance were obtained for all three actinometers. For compounds **1-4**, **15** and **16** consumption of reactant was measured (HPLC), and this value was used for calculating quantum yields. Measurements was done three times in three independent experiments and the mean value is reported.

Steady-State and Time-Resolved Fluorescence Measurements

Steady-state measurements were performed on two different fluorimeters. The samples were dissolved in CH₃CN, or CH₃CN-H₂O (1:1) and the concentrations were adjusted to absorbances of less than 0.1 at the excitation wavelengths of 260, 270 or 280 nm. Solutions were purged with nitrogen for 30 min prior to analysis. Measurements were performed at 20 °C. Fluorescence quantum yields were determined by comparison of the integral of the emission bands with the one of anisole in cyclohexane ($\Phi_f = 0.29$).⁴⁸ Typically, three absorption traces were recorded (and averaged) and three fluorescence emission traces were collected by exciting the sample at three different wavelengths. Three quantum yields were calculated (eq. S1 in the Supporting Information) and the mean value was reported.

Fluorescence decays, collected over 1023 time channels, were obtained on a single photon counter using a light emitting diode for excitation at 260 nm. The instrument response functions, using LUDOX as the scatterer, were recorded at the same wavelengths as the excitation wavelength and had a half width of ≈ 0.2 ns. Emission decays for samples in CH₃CN solutions were recorded at 310 nm for **1** and **2**, and at 320 nm for **3** and **4**. The counts in the peak channel were 2×10^2 for **1** and **3**, and 5×10^2 for **2** and **4**, because the fluorescence intensity was low and further accumulation of data was not possible. The time increment per channel was 0.020 ns. Obtained histograms were fit as sums of exponentials using global Gaussian-weighted non-linear least-squares fitting based on Marquardt-Levenberg minimization implemented in the Fast software package from the instrument. The fitting parameters (decay times and pre-exponential factors) were determined by minimizing the reduced chi-square χ^2 and graphical methods were used to judge the quality of the fit that included plots of the weighted residuals vs. channel number.

Alternatively, a single photon counting setup was used that consisted of 267 nm pulsed light emitting diode with a repetition rate of 10 MHz. The instrument response function of this setup was 250 ps. The time traces (4096 channels) were analyzed by software from the instrument (for more details see the Supporting info.).

Determination of pK_a and pK_a^* for **2 and **4****

UV-vis titration

A solution of compound **2** ($c = 2.72 \times 10^{-4}$ M) or **4** ($c = 2.66 \times 10^{-4}$ M) was prepared in H₂O (120 mL). That solution was titrated with a diluted solution of NaOH until pH 13 was reached. The measurements were performed at 25 °C. The resulting UV-vis spectra were processed by

multivariate nonlinear regression analysis using the SPECFIT program. In the analysis a surface was fit that is defined by all UV-vis spectra from 225 to 350 nm at different pH values.

Fluorescence titration

The titration was performed by mixing a buffer solution (HClO₄, citrate, and phosphate) in a concentration range of 10 to 100 mM to the same volume of CH₃CN (pH from 1.0 to 9.2). The concentrations of **2** and **4** were 6.0×10⁻⁴ M and 7.0×10⁻⁴ M, respectively. In order to get the best spectra, the excitations were performed near the isosbestic point (290 nm for **2** and 295 nm for **4**, the bandwidth of the excitation and emission monochromators were set to 2 nm), so that absorbance in the S₀ was pH independent. The baseline corrected peak maxima found were plotted against the pH value to estimate the pK* values.

Laser Flash Photolysis (LFP)

All LFP studies were performed on a system previously described⁸⁶ using as an excitation source a pulsed Nd:YAG laser at 266 nm (<20 mJ per pulse), with a pulse width of 10 ns. Static cells (7 mm × 7 mm) were used and the solutions were purged with nitrogen or oxygen for 20 min prior to performing the measurements. Absorbances at 266 nm were ~ 0.3-0.5. For the collection of decays at long time scales, a modification of the setup was used, wherein the probing light beam from the Xe-lamp was not pulsed, as previously described.⁷²

Acknowledgement

These materials are based on work financed by the Croatian Foundation for Science (HRZZ, IP-2014-09-6312), the Natural Sciences and Engineering Research Council (NSERC) for CB

(RGPIN-121389-2012) of Canada, the University of Victoria (UVIC) and EPA-Austria. NB and ĐŠ thank dr. K. Mlinarić-Majerski for the useful discussions. NB thanks UVIC for the support, and Professor P. Wan for support and useful discussions.

Supporting information contains: UV-vis and fluorescence spectra of **1-4**, pH titration data for **2** and **4**, selected experimental procedures and results, LFP data and ¹H and ¹³C NMR spectra. This material is available free of charge via the Internet at <http://pubs.acs.org>.

References:

-
- ¹ Rokita, S. E. (Ed.) *Quinone Methides*, Wiley, Hoboken, 2009.
 - ² Freccero, M. *Mini Rev. Org. Chem.* **2004**, *1*, 403-415.
 - ³ Wang, P.; Song, Y.; Zhang, L.; He, H.; Zhou, X. *Curr. Med. Chem.* **2005**, *12*, 2893-2913.
 - ⁴ Basarić, N.; Mlinarić-Majerski, K.; Kralj, M. *Curr. Org. Chem.* **2014**, *18*, 3-18.
 - ⁵ Percivalle, C.; Doria, F.; Freccero, M. *Curr. Org. Chem.* **2014**, *18*, 19-43.
 - ⁶ Wang, H. *Curr. Org. Chem.* **2014**, *18*, 44-60.
 - ⁷ McCracken, P. G.; Bolton, J. L.; Thatcher, G. R. J. *J. Org. Chem.* **1997**, *62*, 1820-1825.
 - ⁸ Modica, E.; Zanaletti, R.; Freccero, M.; Mella, M. *J. Org. Chem.* **2001**, *66*, 41-52.
 - ⁹ Arumugam, S.; Guo, J.; Mbua, N. E.; Friscourt, F.; Lin, N.; Nekongo, E.; Boons, G.-J.; Popik, V. V. *Chem. Sci.* **2014**, *5*, 1591-1598.
 - ¹⁰ Rokita, S. E.; Yang, J.; Pande P.; Greenberg, W. A. *J. Org. Chem.*, **1997**, *62*, 3010-3012.
 - ¹¹ Veldhuyzen, W. F.; Shallop, A. J.; Jones, R. A.; Rokita, S. E. *J. Am. Chem. Soc.* **2001**, *123*, 11126-11132.
 - ¹² Weinert, E. E.; Frankenfield, K. N.; Rokita, S. E. *Chem. Res. Toxicol.* **2005**, *18*, 1364-1370.
 - ¹³ Chatterjee, M.; Rokita, S. E. *J. Am. Chem. Soc.* **1994**, *116*, 1690-1697.

-
- ¹⁴ Zeng, Q.; Rokita, S. E. *J. Org. Chem.* **1996**, *61*, 9080-9081.
- ¹⁵ Pande, P.; Shearer, J.; Yang, J.; Greenberg, W. A.; Rokita, S. E. *J. Am. Chem. Soc.* **1999**, *121*, 6773-6779.
- ¹⁶ Veldhuyzen, W. F.; Pande, P.; Rokita, S. E., A. *J. Am. Chem. Soc.* **2003**, *125*, 14005-14013.
- ¹⁷ Li, V.S.; Kohn, H., *J. Am. Chem. Soc.* **1991**, *113*, 275-283.
- ¹⁸ Han, I.; Russell, D.J.; Kohn, H. *J. Org. Chem.* **1992**, *57*, 1799-1807.
- ¹⁹ Tomasz, M.; Das, A.; Tang, K. S.; Ford, M. G. J.; Minnock, A.; Musser, S. M.; Waring, M. J. *J. Am. Chem. Soc.*, **1998**, *120*, 11581-11593.
- ²⁰ Kralj, M.; Uzelac, L.; Wang, Y.-H.; Wan, P.; Tireli, M.; Mlinarić-Majerski, K.; Piantanida, I.; Basarić, N. *Photochem. Photobiol. Sci.* **2015**, *14*, 1082-1092.
- ²¹ Bolon, D. A. *J. Org. Chem.* **1970**, *35*, 3666-3670.
- ²² Qiao, G. G.-H.; Lenghaus, K.; Solomon, D. H.; Reisinger, A.; Bytheway, I.; Wentrup, C. *J. Org. Chem.* **1998**, *63*, 9806-9811.
- ²³ Dorrestijn, E.; Kranenburg, M.; Ciriano, M. V.; Mulder, P. *J. Org. Chem.* **1999**, *64*, 3012-3018.
- ²⁴ Yato, M.; Ohwada, T.; Shudo, K. *J. Am. Chem. Soc.* **1990**, *112*, 5341-5342.
- ²⁵ Seiler, P.; Wirz, J. *Tetrahedron Lett.* **1971**, *20*, 1685-1686.
- ²⁶ Chiang, Y.; Kresge, A. J.; Zhu, Y. *J. Am. Chem. Soc.* **2002**, *124*, 6349-6356.
- ²⁷ Diao, L.; Yang, C.; Wan, P. *J. Am. Chem. Soc.* **1995**, *117*, 5369-5370.
- ²⁸ Arumugam, S.; Popik, V. V. *J. Am. Chem. Soc.* **2009**, *131*, 11892-11899.
- ²⁹ Lukeman, M.; Wan, P. *J. Am. Chem. Soc.* **2002**, *124*, 9458-9464.
- ³⁰ Basarić, N.; Došlić, N.; Ivković, J.; Wang, Y. H.; Mališ, P.; Wan, P. *Chem. Eur. J.* **2012**, *18*, 10617-10623.
- ³¹ Brousmiche, D.; Xu, M.; Lukeman, M.; Wan, P. *J. Am. Chem. Soc.* **2003**, *125*, 12961-12970.
- ³² Colloredo-Mels, S.; Doria, F.; Verga, D.; Freccero, M., *J. Org. Chem.* **2006**, *71*, 3889-3895.
- ³³ Di Antonio, M.; Doria, F.; Mella, M.; Merli, D.; Profumo, A.; Freccero, M., *J. Org. Chem.* **2007**, *72*, 8354-8360.

-
- ³⁴ Verga, D.; Nadai, M.; Doria, F.; Percivalle, C.; Di Antonio, M.; Palumbo, M.; Richter, S. N.; Freccero, M. *J. Am. Chem. Soc.* **2010**, *132*, 14625-14637.
- ³⁵ Doria, F.; Richter, S. N.; Nadai, M.; Colloredo-Mels, S.; Mella, M.; Palumbo, M.; Freccero, M. *J. Med. Chem.* **2007**, *50*, 6570-6579.
- ³⁶ Nadai, M.; Doria, F.; Di Antonio, M.; Sattin, G.; Germani, L.; Percivalle, C.; Palumbo, M.; Richter, S. N.; Freccero, M. *Biochimie* **2011**, *93*, 1328-1340.
- ³⁷ Doria, F.; Nadai, M.; Folini, M.; Di Antonio, M.; Germani, L.; Percivalle, C.; Sissi, C.; Zaffaroni, N.; Alcaro, S.; Artese, A.; Richter, S. N.; Freccero, M. *Org. Biomol. Chem.* **2012**, *10*, 2798-2806.
- ³⁸ Doria, F.; Nadai, M.; Folini, M.; Scalabrin, M.; Germani, L.; Sattin, G.; Mella, M.; Palumbo, M.; Zaffaroni, N.; Fabris, D.; Freccero, M.; Richter, S. N. *Chem. Eur J.* **2013**, *19*, 78-81.
- ³⁹ Stedman, E. *J. Chem. Soc.* **1927**, 1902.
- ⁴⁰ http://sdbs.db.aist.go.jp/sdbs/cgi-bin/direct_frame_disp.cgi?sdbno=1680
- ⁴¹ Pines, E., *The Chemistry of Phenols*, Rappoport, Z. (Ed.) Wiley, New York, 2003.
- ⁴² Ireland, J. F.; Wyatt, P. A. H. *Adv. Phys. Org. Chem.* **1976**, *12*, 131-221.
- ⁴³ Arnaut, L. G.; Formosinho, S. J. *J. Photochem. Photobiol. A: Chem.* **1993**, *75*, 1-20.
- ⁴⁴ Klöpffer, W. *Adv. Photochem.* **1977**, *10*, 311-358.
- ⁴⁵ Formosinho, S. J.; Arnaut, L. G. *J. Photochem. Photobiol. A: Chem.* **1993**, *75*, 21-48.
- ⁴⁶ Ormson, S. M.; Brown, R. G. *Prog. React. Kinet.* **1994**, *19*, 45-91.
- ⁴⁷ Le Gourrierec, D.; Ormson, S. M.; Brown, R. G. *Prog. React. Kinet.* **1994**, *19*, 211-275.
- ⁴⁸ Montalti, M.; Credi, A.; Prodi, L.; Gandolfi, M.T., In *Handbook of Photochemistry*; CRC Taylor and Francis: Boca Raton, 2006.
- ⁴⁹ Tolbert, L. M.; Solntsev, K. M. *Acc. Chem. Res.* **2002**, *35*, 19-27.
- ⁵⁰ Agmon, N. *J. Phys. Chem. A*, **2005**, *109*, 13-35.
- ⁵¹ Grampp, H.; Maeder, M.; Meyer, C. J.; Zuberbühler, A. D. *Talanta* **1985**, *32*, 95-101.
- ⁵² Grampp, H.; Maeder, M.; Meyer, C. J.; Zuberbühler, A. D. *Talanta* **1985**, *32*, 257-264.

-
- ⁵³ Grampp, H.; Maeder, M.; Meyer, C. J.; Zuberbühler, A. D. *Talanta* **1985**, *32*, 1133-1139.
- ⁵⁴ Brown, W.; Iverson, B.; Anslyn, E.; Foote, C. *Organic Chemistry*, Cengage Learning, Belmont: 2014.
- ⁵⁵ Kanamori, D.; Furukawa, A.; Okamura, T.-A.; Yamamoto, H.; Ueyama, N. *Org. Biomol. Chem.* **2005**, *3*, 1453-1459.
- ⁵⁶ Weinert, E. E.; Dondi, R.; Colloredo-Melz, S.; Frankenfield, K. N.; Mitchell, C. H.; Freccero, M.; Rokita, S. E. *J. Am. Chem. Soc.* **2006**, *128*, 11940-11947.
- ⁵⁷ Shikhmamedbekova, A. Z.; Bairamov, G. B., *Katalit. Prevrashch. Kislorod. i Serosoderzh. Organ. Soedin., Baku*, **1983**, 74-78.
- ⁵⁸ Liu, Q.; Rovis, T. *J. Am. Chem. Soc.* **2006**, *128*, 2552-2553.
- ⁵⁹ Lee, J.; Robinson, G. W.; Webb, S. P.; Philips, L. A.; Clark, J. H. *J. Am. Chem. Soc.* **1986**, *108*, 6538-6542.
- ⁶⁰ Robinson, G. W. *J. Phys. Chem.* **1991**, *95*, 10386-10391.
- ⁶¹ Tolbert, L. M.; Haubrich, J. E. *J. Am. Chem. Soc.* **1994**, *116*, 10593-10600.
- ⁶² Solntsev, K. M.; Huppert, D.; Agmon, N.; Tolbert, L. M. *J. Phys. Chem. A* **2000**, *104*, 4658-4669.
- ⁶³ Wan, P.; Chak, B. *J. Chem. Soc., Perkin Trans. 2* **1986**, *11*, 1751.
- ⁶⁴ Basarić, N.; Cindro, N.; Bobinac, D.; Mlinarić-Majerski, K.; Uzelac, L.; Kralj, M.; Wan, P., *Photochem. Photobiol. Sci.* **2011**, *10*, 1910-1925.
- ⁶⁵ Basarić, N.; Cindro, N.; Bobinac, D.; Uzelac, L.; Mlinarić-Majerski, K.; Kralj, M.; Wan, P., *Photochem. Photobiol. Sci.* **2012**, *11*, 381-396.
- ⁶⁶ Veljković, J.; Uzelac, L.; Molčanov, K.; Mlinarić-Majerski, K.; Wan, P.; Basarić, N., *J. Org. Chem.* **2012**, *77*, 4596-4610.
- ⁶⁷ Van de Water, R. W.; Pettus, T. R. R. *Tetrahedron* **2002**, *58*, 5367-5405.
- ⁶⁸ Cao, S.; Christiansen, R.; Peng, X. *Chem. Eur. J.* **2013**, *19*, 9050-9058.
- ⁶⁹ Krohn, K.; Rieger, H.; Khanbabae, K. *Chem. Ber.* **1989**, *122*, 2323-2330.
- ⁷⁰ Goldstein, S.; Rabani, J. *J. Photochem. Photobiol.* **2008**, *193*, 50-55.

-
- ⁷¹ Kuhn, H. J.; Braslavsky, S. E.; Schmidt, R. *Pure Appl. Chem.* **2004**, *76*, 2105-2146.
- ⁷² Mitchell, R. H.; Bohne, C.; Wang, Y.; Bandyopadhyay, S.; Wozniak, C. B. *J. Org. Chem.* **2006**, *71*, 327-336.
- ⁷³ Chiang, Y.; Kresge, A. J.; Zhu, Y. *J. Am. Chem. Soc.* **2000**, *122*, 9854-9855.
- ⁷⁴ Chiang, Y.; Kresge, A. J.; Zhu, Y. *J. Am. Chem. Soc.* **2001**, *123*, 8089-8094.
- ⁷⁵ Chiang, Y.; Kresge, A. J.; Zhu, Y. *J. Am. Chem. Soc.* **2002**, *124*, 717-722.
- ⁷⁶ Richard, J. P.; Toteva, M. M.; Crueiras, J. *J. Am. Chem. Soc.* **2000**, *122*, 1664-1674.
- ⁷⁷ Toteva, M. M.; Richard, J. P. *Adv. Phys. Org. Chem.* **2011**, *45*, 39-91.
- ⁷⁸ Ottosson, H., *Nature Chem.* **2012**, *4*, 969-970.
- ⁷⁹ Rosenberg, M.; Dahlstrand, C.; Kilså, K.; Ottosson, H. *Chem. Rev.* **2014**, *114*, 5379-5425.
- ⁸⁰ Wang, H.; Wahi, M. S.; Rokita, S. E. *Angew. Chem. Int. Ed.* **2008**, *47*, 1291-1293.
- ⁸¹ Wang, H.; Rokita, S. E. *Angew. Chem. Int. Ed.* **2010**, *49*, 5957-5960.
- ⁸² Rossiter, C. S.; Modica, E.; Kumar, D.; Rokita, S. E. *Chem. Commun.* **2011**, *47*, 1476-1478.
- ⁸³ Houben, J.; Weyl T., (Eds) *Methoden der Organische Chemie*, Vol. 11/1, Georg Thieme Verlag: Stuttgart, 1957.
- ⁸⁴ Tamiselvi, A.; Muyesh, G. *Inorg. Chem.* **2011**, *50*, 749-756.
- ⁸⁵ Škalamera, Đ.; Mlinarić-Majerski, K.; Martin-Kleiner, I.; Kralj, M. Wan, P. Basarić, N. *J. Org. Chem.* **2014**, *79*, 4390.
- ⁸⁶ Liao, Y.; Bohne, C. *J. Phys. Chem.*, **1996**, *100*, 734-743.